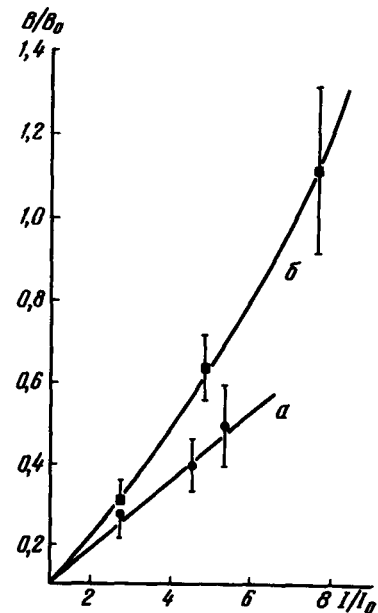


conversion from density to brightness (Fig. 3) than that of our earlier paper [4].

Fig. 3. Relative brightnesses of the proton tracks,  $B/B_0$  ( $B_0$  - average brightness of tracks with ionization  $I_0 = 1.2 I_{\min}$ ) at pulse durations  $\tau$  and  $\tau_{III}$ .



In conclusion, the authors thank A. I. Alikhanyan, I. M. Vasilevskii, A. F. Pisarev, A. A. Tyapkin, and G. E. Chikovani for interest, collaboration, and useful discussions, and also A. F. Filozov and R. O. Sharkhatunyan for direct help in performing the experiment and reducing the material.

- [1] E. Gygi and F. Schneider, Preprint CERN AR/Int, GS/65-1.
  - [2] G. E. Chikovani, V. N. Roinishvili, and V. A. Mikhailov, Communications (Soobshcheniya), Georgian Academy of Sciences, 35, 539 (1964).
  - [3] E. K. Bjornerud, Rev. Sci. Instr. 26, No. 9, (1955).
  - [4] T. L. Asatiani, K. A. Gazarian, V. N. Zhmirov, E. M. Matevosian, A. A. Nazarian, and R. O. Sharkhatunian, Preprint E-2324, JINR, Dubna, 1965.
- \*The photograph (Fig.1) was left out of the original Russian issue - Transl.

#### QUANTUM NOISE IN PARAMETRIC LIGHT AMPLIFIERS

S. A. Akhmanov, V. V. Fadeev, R. V. Khokhlov, and O. N. Chunaev  
 Physics Department, Moscow State University  
 Submitted 4 May 1967  
 ZhETF Pis'ma 6, No. 4, 575-578 (15 August 1967)

1. We report in this communication the results of an experiment in which we registered directly the intrinsic (spontaneous) noise of a parametric amplifier (see [1]) operating in the visible part of the optical spectrum ( $0.5 - 0.6 \mu$ ).<sup>\*</sup> In laser terminology, we are dealing with parametric "luminescence" and "superluminescence," which have a number of interesting features.

A block diagram of the experimental setup used in our experiments is shown in Fig. 1. We used in the amplifier a KDP crystal 4 cm long (KDP-III); the pumping was with the third harmonic of a neodymium laser ( $\lambda_3 = 0.353 \mu$ ) produced in crystals KDP-1 and KDP-2 by cascade frequency conversion [2]. The maximum pump power density was about  $70 \text{ MW/cm}^2$ ; the divergence was  $7'$ ; the radiation contained approximately 10 spectral lines (modes). The amplifying

crystal was so oriented that the pump excited in it the extraordinary wave; the crystal faces were perpendicular to the direction along which the one-dimensional synchronous interaction between the pump wave and the waves  $\lambda_2 = 0.53 \mu$  (ordinary) and  $\lambda_1 = 1.06 \mu$  (extraordinary), i. e., interaction of the form  $\gamma_e(\omega_1) + \gamma_o(\omega_2) \neq \gamma_e(\omega_3)$ ; the angle  $\theta$  between the sample axis and the optic axis of the crystal was in this case  $\theta_o^{3\omega-\omega} = \theta_o^{\omega+\omega} - 0^\circ 20'$ , \*\* where  $\theta_o^{\omega+\omega}$  is

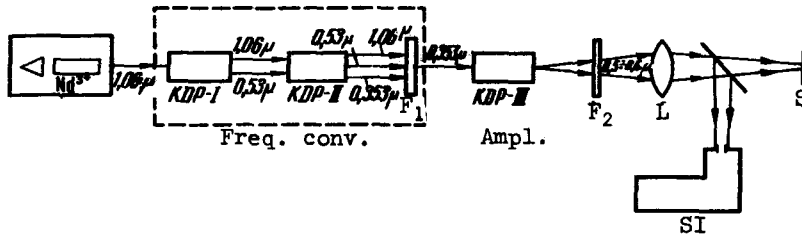


Fig.1. Diagram of experimental setup. F - filters, L - lens of focal length  $f = 10 \text{ cm}$ ; S - screen (or photographic film) in the focal plane of the lens L; SI - spectral instrument (ISP-51 spectrograph or ZMR-3 monochromator with photomultiplier).

the synchronism angle for second-harmonic generation in a neodymium laser (interaction  $\gamma_e(\omega) + \gamma_o(\omega) \neq \gamma_o(2\omega)$ ). The spatial structure of the output signal in the far field was photographed on a film placed in the focal plane of the lens (focal distance  $f = 10 \text{ cm}$ ); the frequency spectrum was analyzed with the aid of narrow-band interference filters, and also with the IS ISP-51 spectrograph; the intensity was estimated by photometry of the photographs and comparison with calibrated light at  $\lambda = 0.53 \mu$ , and was also measured with a photomultiplier (in which case the spectrograph was replaced by a mirror monochromator).

3. Illustrative information concerning the characteristics of the spontaneous noise is gained by observing the angular structure of the light flux emerging from the amplifier at different orientations of the crystal relative to the pump beam (we varied the angle  $\theta_3$  between the pump beam and the crystal optic axis). Figure 2a \*\*\* shows a photograph obtained under conditions when a weak signal at  $\lambda_1 = 1.06 \mu$  was fed to the input of the crystal KDP-III besides the pump signal, and  $\theta_3 = \theta_o^{3\omega-\omega} + 1^\circ 30'$ . The bright spot, the ring, and the arc are connected with the generation of the supplementary wave,  $\lambda_2 = 0.53 \mu$ , respectively for: (a) - one-dimensional non-synchronous interaction of the waves  $\lambda_3$  and  $\lambda_1$ ; (b) - two-dimensional synchronous interaction (phase velocities matched for noncollinear beams) between the direct pump wave and the scattered radiation with  $\lambda_1$  - the weak scattering was unavoidable because of the presence of defects on the crystal surfaces etc.(circle); (c) - synchronous one-dimensional interaction of the scattered waves of the signal and pump (arc, along which  $\theta_3 = \theta_o^{3\omega-\omega}$  is constant). The weak background, which is clearly seen in the photograph, is the spontaneous emission. At a fixed pump power, its intensity does not depend on the neodymium-laser emission penetrating through the filter  $F_1$  at the input to the crystal KDP-III.

The spontaneous-noise spectrum at the amplifier output is quite broad; we registered in our experiments components in the  $0.5 - 0.58 \mu$  band (with this, the wavelength of the corresponding spontaneous emission at the mirror frequency relative to  $\omega_3/2$  varied between  $1.21$  and  $0.9 \mu$ ). Observation of the angle structure of the spontaneous noise through interference filters has shown that the equal-frequency curves are circles whose diameter increases with decreasing wavelength  $\lambda_2$ . The angle structure of the spontaneous noise at a fixed wavelength can be varied by varying the crystal orientation. Characteristic photographs for  $\lambda_2^1 = 0.557 \mu$

and different  $\theta_3$  are shown in Fig. 2b. We see that with decreasing  $\theta_3$  the diameter of the ring decreases; the ring contracts to a point at a certain angle  $\theta_3 = \theta_0(\lambda_2^1)$  and when  $\theta_3 < \theta_0(\lambda_2^1)$  the intensity of the spontaneous emission at  $\lambda_2^1$  greatly decreases and this emission becomes difficult to observe.

The foregoing results obviously indicate that the spontaneous noise is generated in the crystal, in the general case, as a result of the two-dimensional synchronous interaction between the "noise" waves and the direct pump wave (cf. Fig. 2a; the interaction between the spontaneous noise and the scattered pump wave gives a much weaker effect if the scattering is small). The foregoing is illustrated by the spectrograms of Fig. 3 \*\*\* (spectrograph slit width 0.4 mm). The vertices of the arcs correspond here to one-dimensional interactions of the form  $\gamma_e(\omega_1) + \gamma_o(\omega_2) \neq \gamma_e(\omega_3)$ , and the branches facing the violet region correspond to two-dimensional interactions. Comparison of the experimental data concerning the space-frequency structure of the spontaneous noise with the calculated dependences of the synchronous frequencies on the direction in the crystal offer evidence of their good agreement.

4. The measured dependence of the spontaneous noise power  $P_n$  on the pump power  $P_3$  turned out to be nearly linear up to a pump intensity  $S_3 = 45 \text{ MW/cm}^2$ . At higher intensities the conversion rate ( $dP_n/dP_3$ ) increases noticeably. At  $S_3 = 40 \text{ MW/cm}^2$  the spontaneous-noise power at  $\lambda_2 = 0.557 \mu$  in a 50-Å band (the pass band of the interference filter) was about  $10^{-4} \text{ W}$ , and the power density at the focal plane of a lens with 10 cm focus was  $S_{nf} \approx 0.4 \text{ W/cm}^2$ . At the same pump intensity, the parametric gain of the signal at  $\lambda_1 = 1.06 \mu$  in the same crystal (KDP-III) was  $G = 3$ . A theoretical estimate of the noise power density in the focal plane of a lens with  $f = 10 \text{ cm}$ , based on a quantum-mechanical calculation of the decay of the pump photons (see [3, 4], yields  $S_{nf} = 0.7 \text{ W/cm}^2$ .

5. It was not our intent to study in detail in our experiments the spatial and temporal coherence of the spontaneous noise; such investigations are difficult to carry out in the described apparatus, owing to the multimode character of the pump. Measurements similar to those described are now under way with single-mode pumping.

It should be noted that parametric "luminescence" can be observed in gas-laser beams; such an experiment was performed in our laboratory by D. P. Krindach and D. N. Klyshko, who used an argon laser and an  $\text{LiNbO}_3$  crystal.

We are grateful to D. N. Klyshko for useful discussions of the results and to I. A. Yuzevovich for help with the measurements.

- [1] S. A. Akhmanov and R. V. Khokhlov, UFN 88, 439 (1966), Sov. Phys.-Uspekhi 9, 210 (1966).
- [2] S. A. Akhmanov, A. I. Kovrigin, D. S. Piskarskas, and R. V. Khokhlov, ZhETF Pis. Red. 2, 223 (1965), JETP Lett. 2, 141 (1965).
- [3] I. P. Gordon, W. H. Louisell, and L. R. Walker, Phys. Rev. 129, 481 (1963).
- [4] D. N. Klyshko, ZhETF Pis. Red. 6, 490 (1967), JETP Lett. 6, 23 (1967).

\* Preliminary results of the experiment were reported at the Symposium on Modern Optics, 22-24 March 1967, New York.

\*\* The angles  $\theta_o$  (with subscript "o") correspond to one-dimensional interactions.

\*\*\* The photographs referred to here (Figs. 2 and 3) were left out of the original Russian issue. They may be included as errata in a future issue. - Transl.

Vol. 6, No. 4. The following photographs were left out of the earlier edition of the Russian original and were not included in the translated version:

Article by T. L. Asatiani et al, (p. 83):

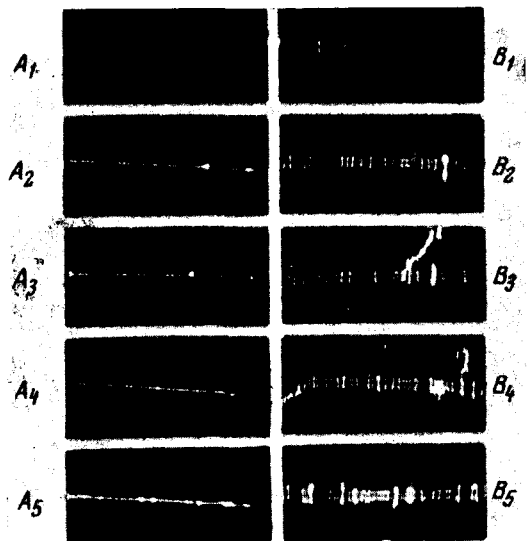


Fig. 1. Photographs of proton tracks in two projections at different energies in the case of a high-voltage pulse duration  $\tau_{III}$ :

$$A_1, B_1 - I/I_{\min} = 1.2; A_2, B_2 - I/I_{\min} = 3.4;$$

$$A_3, B_3 - I/I_{\min} = 5.4; A_4, B_4 - I/I_{\min} = 6.3;$$

$$A_5, B_5 - I/I_{\min} = 8.5.$$

Fig. 2. Space structure in far field: a - emission at difference wavelength  $\lambda_2 = 0.53 \mu$  obtained by mixing the pump and signal at  $\lambda_1 = 1.06 \mu$  (bright spot, ring, and arc) and spontaneous noise (background); b - spontaneous noise passed through interference filter at  $\lambda = 5570 \pm 25 \text{ \AA}$ ; photograph obtained by successive superposition on a single frame of photographs taken at  $\theta_3 = \theta_0^{3\omega - \omega} + 5^\circ 20'$  (outer ring),  $\theta_3 = \theta_0^{3\omega - \omega} + 4^\circ 20'$ , and  $\theta_3 = \theta_0^{3\omega - \omega} + 4^\circ 00'$  (two rings coalescing into a single internal one).

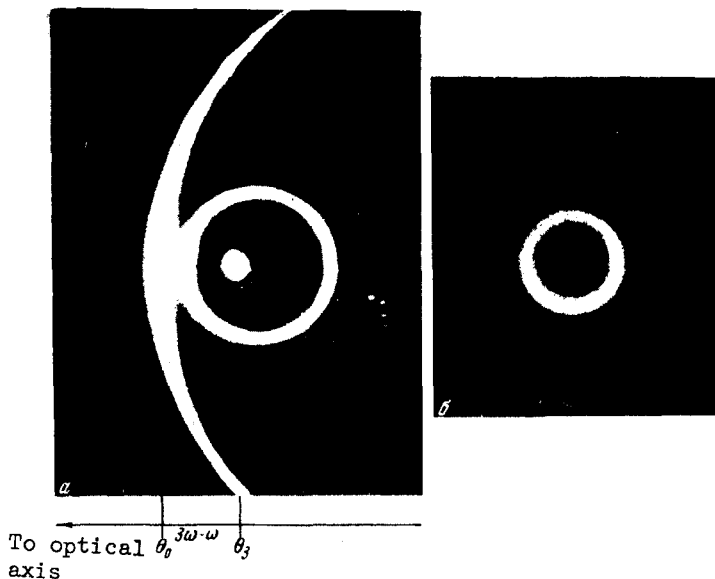
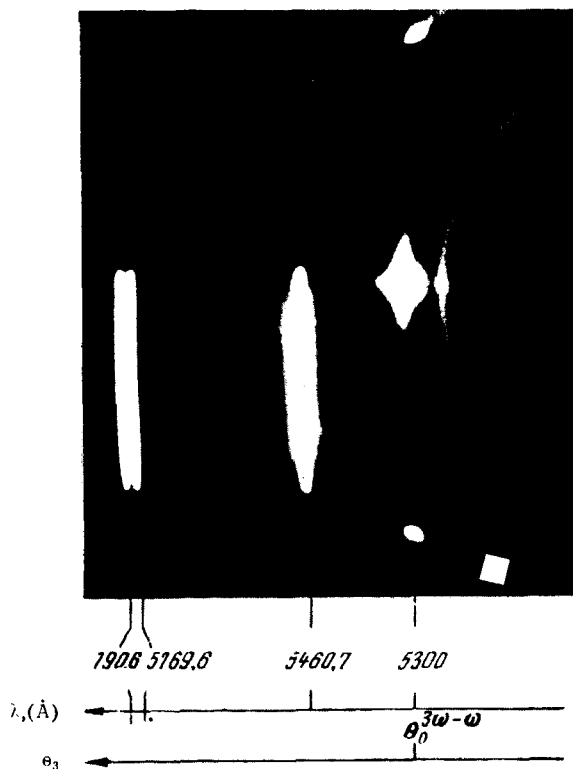


Fig. 3. Spectrograms of spontaneous noise, obtained by superimposing on one frame three spectrograms obtained at angles  $\theta_3 - \theta_0^{3\omega - \omega}$  equal to  $6^\circ 30'$  (a),  $2^\circ 55'$  (b), and  $0^\circ 35'$  (c) (arcs from left to right). The reference lines were obtained with a mercury lamp.



Article by V. A. Atsarkin et al. (p. 88):

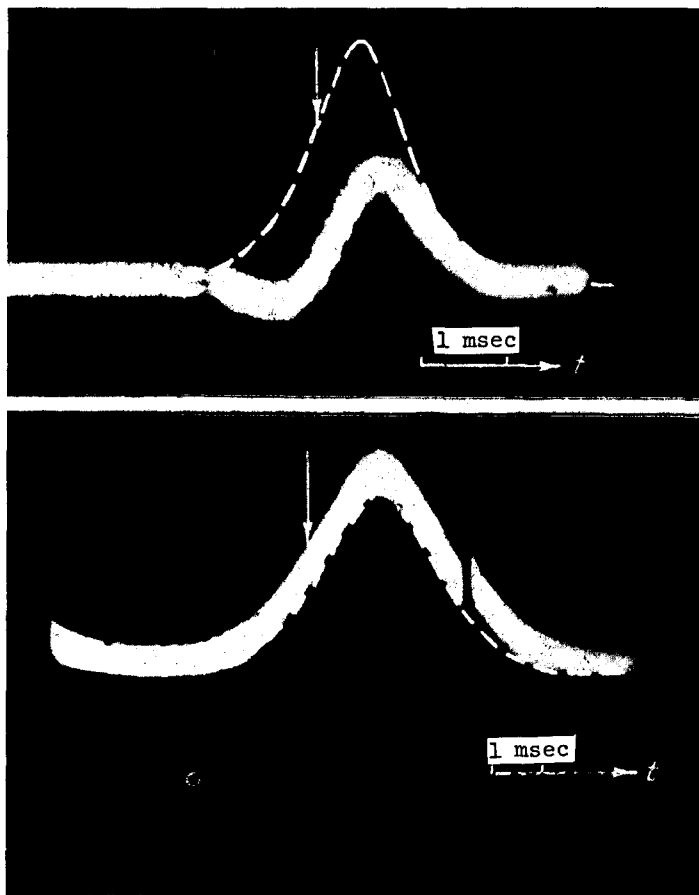


Fig. 2. Oscillograms of EPR line at not-strictly resonant saturation. The notation is the same as in Fig. 1. The magnetic field increases with time in the upper figure and decreases in the lower figure.